Optics Communications 284 (2011) 4782–4788

Contents lists available at ScienceDirect

Optics Communications

journal homepage: www.elsevier.com/locate/optcom

# Study on inverse taper based mode transformer for low loss coupling between silicon wire waveguide and lensed fiber

Guanghui Ren, Shaowu Chen *, Yongpeng Cheng, Yao Zhai

*State Key Laboratory on Optoelectronics, Institute of Semiconductors, Chinese Academy of Sciences, Beijing 100083, China*

ARTICLE INFO

*Article history:*
Received 15 July 2010
Received in revised form 20 December 2010
Accepted 30 May 2011
Available online 12 June 2011

*Keywords:*
Integrated optics
Inverse taper
BPM
Mode transformer

ABSTRACT

We have simulated the coupling loss of three types of Inverse Taper and taper-lensed fiber using three dimensional (3D) semi-vectorial beam propagation methods (BPM) respectively. Our results showed that the performances of exponential inverse taper and quadratic inverse taper were better than the commonly used linear inverse taper. Especially, for TM mode the improvement in the reduction of devices size is 53% and 136% for exponential and quadratic inverse taper compared with the linear inverse taper.



## 1. Introduction

The past decades have witnessed the fast development of Photonics Integrated Circuits (PICs) which is considered to be one of the most powerful platforms for next-generation on-chip interconnection and information processing. Specifically, the silicon based sub-micron waveguide (also known as "silicon wire waveguide") components and devices are commonly deemed as the most potential candidate for PICs applications because they support high density integration and low power consumption. Nowadays many silicon wire waveguides based components that are required to realize PICs have reached a good level of maturity both in theory and in fabrication. However, the coupling loss between silicon wire waveguide and optical fiber which is used to couple in/out light in most cases is so high that it has become one of the most important issues to overcome.

To solve this problem, a mode transformer is needed to serve as a coupler to reduce the mode mismatch coupling loss between silicon wire waveguide and optical fiber. Up to now, several approaches have been proposed such as grating couplers [1–7], prism couplers [8], graded-index coupler [9] and inverse taper couplers [10–16]. The first method, although, can reach high coupling efficiency, say, 55% according to recent report, its operation bandwidth at 1dB is only 50nm. Although, Dual Grating-Assisted Directional Coupler, reported by Goran Z. Masanovic [7], can reach a coupling efficiency as high as 90%, its fabrication is too complicated for practical applications in terms of cost effectiveness. The prism couplers have the same problem as the grating couplers. While the graded-index couplers have wide operation bandwidth, their coupling efficiency cannot reach the requirement of PICs. Also, the fabrication of graded-index coupler is quite complicated. The inverse taper couplers have been proposed several years ago and shown some advantages; while only linear inverse tapers have been designed and fabricated. Although some of them demonstrated high coupling efficiency, most of them are covered by two layer oxide [14] or polymers [16], or adopting three-dimensional structure [17] which needs gray lithography and is not compatible with standard CMOS process.

In this paper, we have designed three types of inverse tapers, i.e. Linear Inverse Taper, Exponential Inverse Taper, and Quadratic Inverse Taper, and given the detailed comparison of their performances. Based on the simulations and analysis, the optimization for inverse taper has been performed. As demonstrated below, the optimization for the inverse taper shape, such as exponential or quadratic inverse taper, can improve the performances. This paper is organized as follows: In Section 2 the coupling model and the gradient line shapes of three types of inverse tapers are presented. Section 3 introduces the numerical model. The simulation results and analysis of three types of inverse tapers are explored in Section 4. Finally, we summarize our paper.

## 2. Coupling model and inverse taper based mode transformer design

The coupling model under simulation is shown in Fig. 1, which consists of a taper-lensed fiber coupled with a silicon wire waveguide via an inverse taper functioned as a mode transformer. All of the inverse tapers and silicon wire waveguide designed in this paper are based on silicon-on-insulator (SOI) wafer with 0.34 μm top silicon

* Corresponding author.
*E-mail address:* swchen@semi.ac.cn (S. Chen).

0030-4018/$ – see front matter © 2011 Elsevier B.V. All rights reserved.
doi:10.1016/j.optcom.2011.05.072

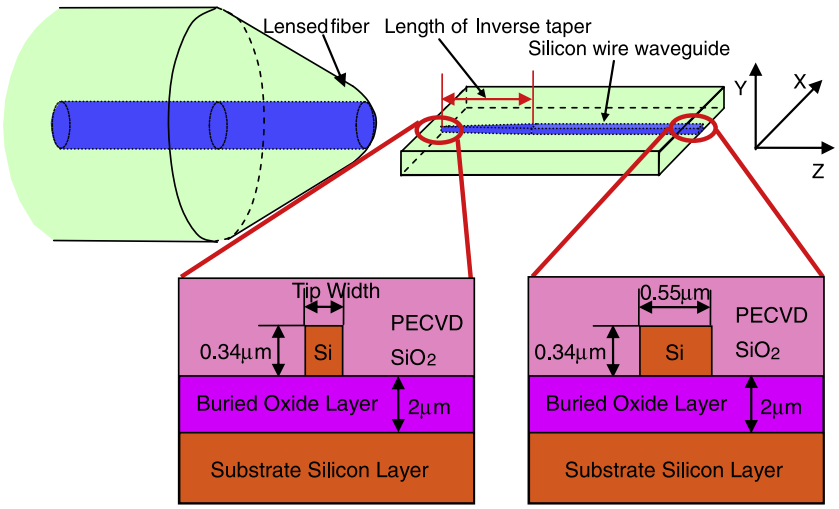


**Fig. 1.** Coupling model between taper-lensed fiber and inverse taper; the insertion are cross sectional schematic of inverse taper tip and the embedded silicon wire waveguide (not to scale).

layer and 2 μm buried oxide layer. The silicon wire waveguide is designed as an embedded waveguide with waveguide height 0.34 μm and width 0.55 μm.

(1) Taper-lensed fiber
In our simulation, we have designed the taper-lensed fiber that can reproduce the performance of the taper-lensed fiber used in our laboratory. It is shown as Fig. 1.
The radius of the fiber core is 4μm, with its index 1.47, and its cladding radius is 125 μm, having 0.01 index difference compared with that of fiber core. The taper length is 58.5 μm, with 90° taper angle. The tip of taper-lensed fiber is designed as an ellipsoid, with its long axis 8 μm and short axis 5 μm, which can focus the light it conveys. In order to insure our design, we have simulated the propagation of light in the taper-lensed fiber. The simulation result is shown as Fig. 2 (the length of the tape-lensed fiber is 200 μm). As we have expected, the light convergence can be realized. At the focus point, the spot size (2.56 μm) and the working distance (14.3 μm) are precisely the same as those of the taper-lensed fiber used in our laboratory (spot size = 2.5 ± 0.25 μm, working distance = 14 ± 2 μm). Only using this precisely designed taper-lensed fiber can we reproduce the performance of the one that was used in our lab accurately.

(2) Inverse taper
The parameters that affect the performance of inverse taper are gradient line shape, taper tip width, taper length, operation wavelength, and misalignment. We have designed three different Inverse Tapers; they are Linear Taper, Exponential Taper and Quadratic Taper, which is described respectively as below:

A. Linear inverse taper
Its taper gradient line shape function is

$$z' = \frac{z - z_0}{z_1 - z_0} \qquad f(z') = z' \tag{1}$$

where $z_0$ and $z_1$ are the Z coordinates of the starting and ending vertices respectively, and $z$ is the actual Z coordinate along the waveguide relative to the starting vertex. It is shown as Fig. 3(a).

B. Exponential inverse taper
Its taper gradient line shape function is

$$z' = \frac{z - z_0}{z_1 - z_0} \qquad f(z') = \frac{e^{z'} - 1}{e - 1} \tag{2}$$

where $z_0$ and $z_1$ are the Z coordinates of the starting and ending vertices respectively, and $z$ is the actual Z coordinate along the waveguide relative to the starting vertex. It is shown as Fig. 3(b).

C. Quadratic inverse taper
Its taper gradient line shape function is

$$z' = \frac{z - z_0}{z_1 - z_0} \qquad f(z') = z'^2 \tag{4}$$

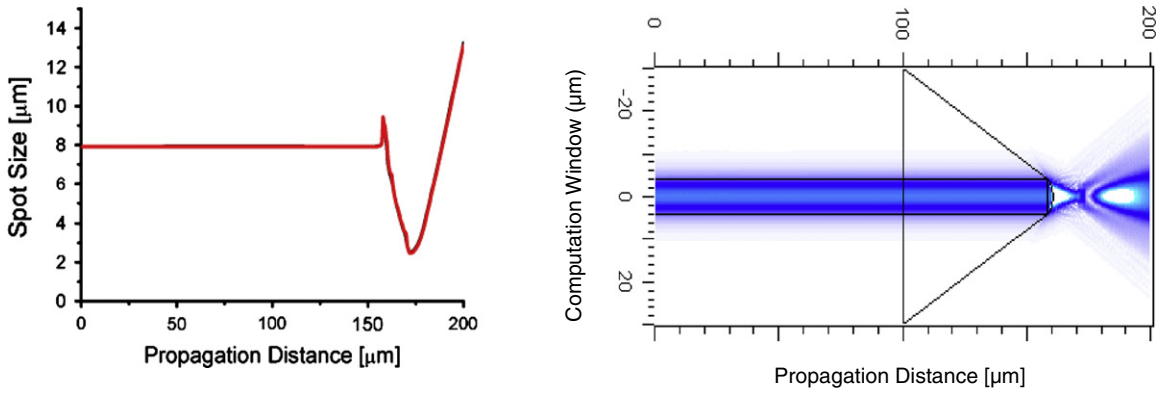


**Fig. 2.** The variation of spot size in taper-lensed fiber along propagation direction and the propagation of light in the taper-lensed fibe.


**Fig. 3.** The inverse taper (a) linear inverse taper (b) exponential inverse taper (c) quadratic inverse taper (not to scale).

where $z_0$ and $z_1$ are the Z coordinates of the starting and ending vertices respectively, and $z$ is the actual Z coordinate along the waveguide relative to the starting vertex. It is shown as Fig. 3(c).

(3) Coupling efficiency definition

The coupling efficiency between taper-lensed fiber and inverse taper is determined by the overlap integration of their optical fields, as expressed below.

$$\eta(z) = \frac{\left|\int_{-\infty}^{+\infty}\int_{-\infty}^{+\infty} \overrightarrow{E_1}(x,y,z)\bullet \overrightarrow{E_f}(x,y,z)dxdy\right|^2}{\int_{-\infty}^{+\infty}\int_{-\infty}^{+\infty} \overrightarrow{E_1}(x,y,z)\bullet \overrightarrow{E_1^*}(x,y,z)dxdy\int_{-\infty}^{+\infty}\int_{-\infty}^{+\infty} \overrightarrow{E_f}(x,y,z)\bullet \overrightarrow{E_f^*}(x,y,z)dxdy} \quad (5)$$

Where $E_1(x, y, z)$ is the electrical field at the tip of inverse taper, and $E_f(x, y, z)$ is the electrical field at the focus plane of taper-lensed fiber. Besides, in our simulation, the propagation loss of taper-lensed fiber, the loss of mode mismatch, the reflection loss between the air and device and the propagation loss of inverse taper have been considered. So, the total coupling efficiency (in dB) is expressed as below:

$$\text{Total coupling efficiency (dB)} = 10 \times log_{10}(\alpha\bullet\eta) \quad (6)$$

Where $\alpha$ is the coefficient that represent the propagation loss of taper-lensed fiber plus inverse taper, and the reflection loss between air and device facet.

## 3. Numerical modeling introduction

The 3D semi-vectorial beam propagation method (BPM) has been utilized for the numerical analysis of the coupling between inverse taper and taper-lensed fiber. The 3D semi-vectorial BPM actually simplifies the coupled equations for the transverse components of the field (Ex and Ey). In this case, the transverse field components are decoupled. Pin-Chia Lee [18] has demonstrated that semi-vectorial BPM is valid for most cases, including coupling case. In our simulation, we have analyzed TE mode and TM mode respectively and find that there is no coupling between them. So, it is reasonable to adopt semi-vectorial BPM in our simulation. Also, in our simulation, the full transparency boundary condition has been used, due to the fact that the field has actually faded away when it spreads out laterally as far as 15 μm. The computation window is 30μm × 30μm, and the grid size is 0.05 μm.

## 4. Simulation results and discussion

The fundamental factors that lead to the high coupling loss between the taper-lensed fiber and the inverse taper are the effective index and the mode size mismatch. So, in order to cut down the high coupling loss, the effective index and the mode size of the inverse tapers should be much more alike with that of the taper-lensed fiber.

In this section, we have analyzed the parameters, i.e. taper tip width, taper length, taper gradient line shape function, the operation wavelength and the misalignment of inverse taper and taper-lensed fiber; and they are all probable factors affecting the performances of inverse tapers. Among them, the first two are the intrinsic factors that affect the performances of the inverse tapers, while the other two are the environmental factors.

(1) The effect of inverse taper tip width

The tip width mainly affects the effective index of the inverse taper. It can be illustrated in Fig. 4. From this graph, we can see that with the increasing of the taper tip width, the effective index grows gradually. This is because of the fact that the confinement of the waveguides become larger and larger with the increasing of the taper tip width, which in turn leads to the decreasing of the delocalization of the field in the waveguides.

In this section, the inverse taper length is fixed at 300 μm because the three types of inverse tapers exhibit no significant changes for the length over 100 μm. And, the taper tip width varies from 0.01 μm to 0.55 μm, followed by a 100 μm long and 0.55 μm wide embedded waveguide. The simulation results of the dependence of the coupling loss on tip width are shown as below:

A. Linear inverse taper

It can be illustrated from Fig. 5 that there is an optimal taper tip width not only for TE mode but also for TM mode. For TE mode the optimal tip width is 0.08 μm, while 0.04 μm for TM mode. This is because of that the effective index and the mode size mismatch between the inverse taper and the taper-lensed fiber

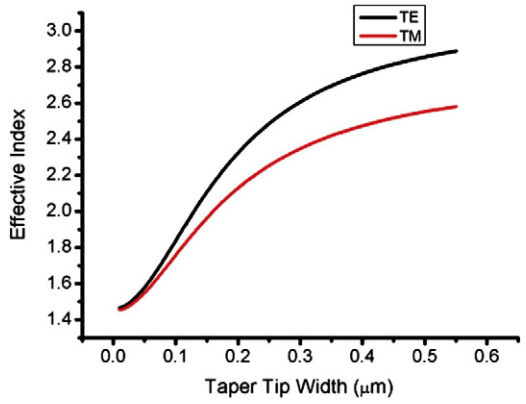


**Fig. 4.** The dependence of the effective index on the taper tip width.

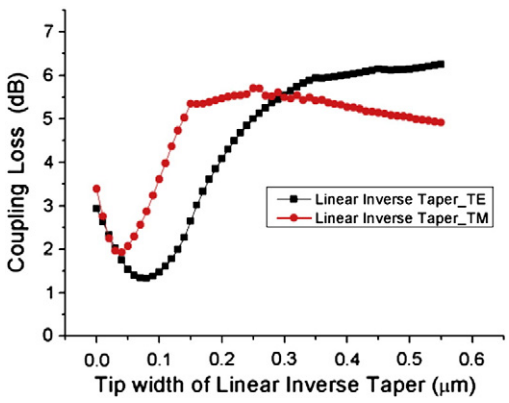


**Fig. 5.** The effect of taper tip width on the coupling loss of linear inverse taper.

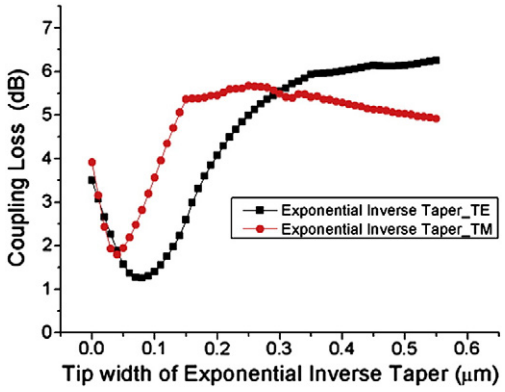


**Fig. 6.** The effect of taper tip width to coupling loss for exponential inverse taper.

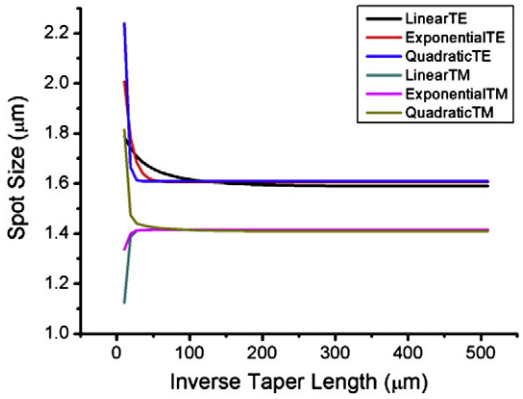


**Fig. 8.** The dependence of spot size on the taper length.

is smallest at this tip width. The coupling efficiency tendency versus tip width is almost the same for TE and TM mode except there is a slight increase for TM mode when the tip width is larger than 0.26 μm. The minor coupling loss is 1.33 dB for TE mode while 1.93 dB for TM mode. When the taper tip width is larger than 0.3 μm, the coupling loss for TM mode is smaller than that for TE mode. This difference between TE and TM mode is introduced by the fact that the polarization of TE mode is parallel to the direction of taper width which varies gradually while the polarization of TM mode parallel to the direction of taper height which is fixed at 0.34 μm. So, when the tip width is larger than 0.3 μm, the confinement factor of inverse taper for TE mode becomes larger than that of TM mode, as a result, the delocalization of TE mode becomes weaker than that of TM mode, As we know, the weaker delocalization, the smaller mode profile, and in turn, the smaller mode profile matching with that of the taper-lensed fiber. Besides, when the tip width is larger than 0.3 μm for TE mode and 0.15 μm for TM mode, the coupling efficiency almost keeps stable. This is because of the fact that in that case the effective index changes slightly and the index mismatch almost keeps at the same level.

B. Exponential inverse taper

We can obtain the minor coupling loss point for exponential inverse taper from Fig. 6, 1.26 dB at 0.08 μm tip width for TE mode and 1.79 dB at 0.04 μm tip width for TM mode. When tip width is smaller or larger than the minor coupling loss points, the coupling loss increases sharply. The difference between TE and TM mode is the same as that of linear inverse taper.

C. Quadratic inverse taper

Fig. 7 shows the same tendency for both the TE mode and TM mode as that of linear and exponential inverse tapers. The minor coupling loss point located at 0.08 μm for TE mode with 1.19 dB coupling loss, while 1.75 dB at 0.04 μm for TM mode.

(2) The effect of inverse taper length

The inverse taper length mainly affects the mode size. It can be illustrate by the following graph. It can be seen from Fig. 8 that the spot size of TE mode is larger than that of TM mode, because the delocalization for TE mode which is parallel to the width of the inverse tape is much stronger than that for TM mode which is perpendicular to the width of the inverse taper. Besides, the spots sizes of the quadratic inverse taper change more dramatically than that of exponential and linear inverse taper. This is because of that the taper angle which is defined as arctan{[(embedded waveguide width) − (inverse taper tip width)]/[2*(inverse taper length)]} for the quadratic inverse taper is much larger than that of the other two types, which in turn transform the mode size more quickly and largely.

In this section, the affection of inverse taper length to coupling efficiency has been studied. We fixed inverse taper tip width at 0.08 μm for TE mode and 0.04 μm for TM mode for the sake of almost the same influence of inverse taper tip width to coupling efficiency for all the three inverse tapers.

A. Linear inverse taper

From Fig. 9 we can see that with the increase of inverse taper length the coupling loss descends dramatically at first and then decreases slowly when the taper length is longer than 250 μm (1.37 dB) for TE mode and 200 μm (2.13 dB) for TM mode. The reason why coupling loss for TM mode are higher than that for TE mode at any taper length is that the coupling loss for TM mode with 0.04 μm taper tip width is higher than that for TE

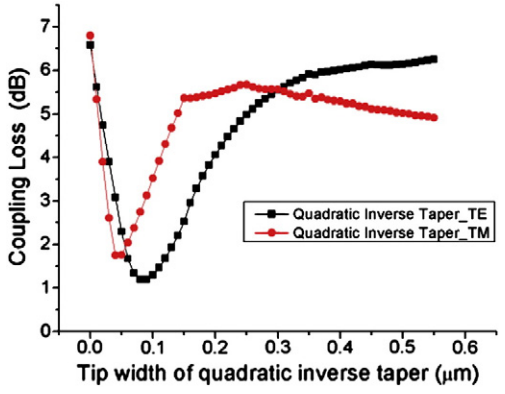


**Fig. 7.** The effect of taper tip width to coupling loss for quadratic inverse taper.

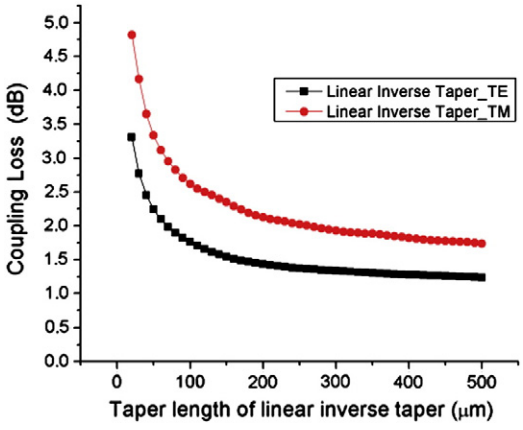


**Fig. 9.** The effect of inverse taper length to coupling loss for linear inverse taper.

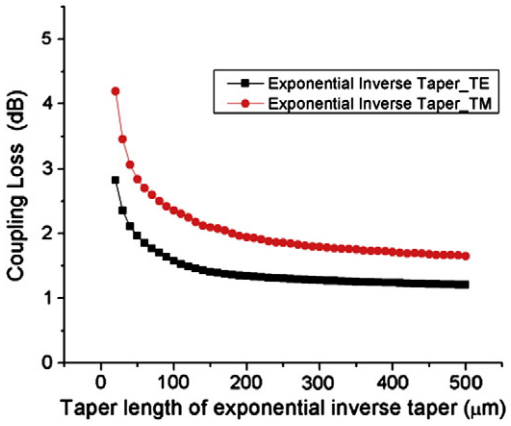


**Fig. 10.** The effect of inverse taper length to coupling loss for exponential inverse taper.

mode with 0.08 μm taper tip width. Besides, with varied taper length, the TE mode field delocalizes more dramatically than that of the TM mode, which enlarges the mode size of the inverse taper, and in turn strengthens the coupling between inverse taper and taper-lensed fiber. Besides, when the taper length if larger than 250 μm for TE mode (200 μm for TM mode) the coupling loss almost keeps stable, which is because of the fact that the spot size do not change greatly and in turn lead to the steady spot size mismatch with that of the taper-lensed fiber.

B. Exponential inverse taper

The information conveyed by Fig. 10 is that the coupling efficiency increases rapidly at first and reaches a relatively steady level when the taper length is larger than 170 μm (1.37 dB) for TE mode and 140 μm (2.12 dB) for TM mode. The difference of coupling loss for TE mode and TM mode is the same as that of linear inverse taper.

C. Quadratic inverse taper

The tendency of coupling efficiency versus inverse taper length is the same as that of linear and exponential inverse taper, which can be seen in Fig. 11. The only difference is the steady point, 170 μm (1.39 dB) for TE mode and 150 μm (1.87 dB) for TM mode.

(3) The effect of inverse taper function

Fig. 12(a) tells us that with the fixed taper length 300 μm when the tip width is smaller than 0.08 μm for TE mode (0.04 μm for TM mode) the coupling loss of linear inverse taper is lower than that of exponential and quadratic inverse taper. This is because the propagation loss of linear taper is smaller than that of exponential and quadratic taper [19]. Under such situation, the

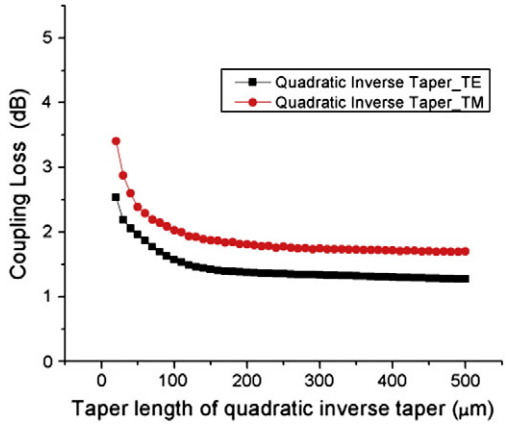


**Fig. 11.** The effect of inverse taper length to coupling loss for quadratic inverse taper.

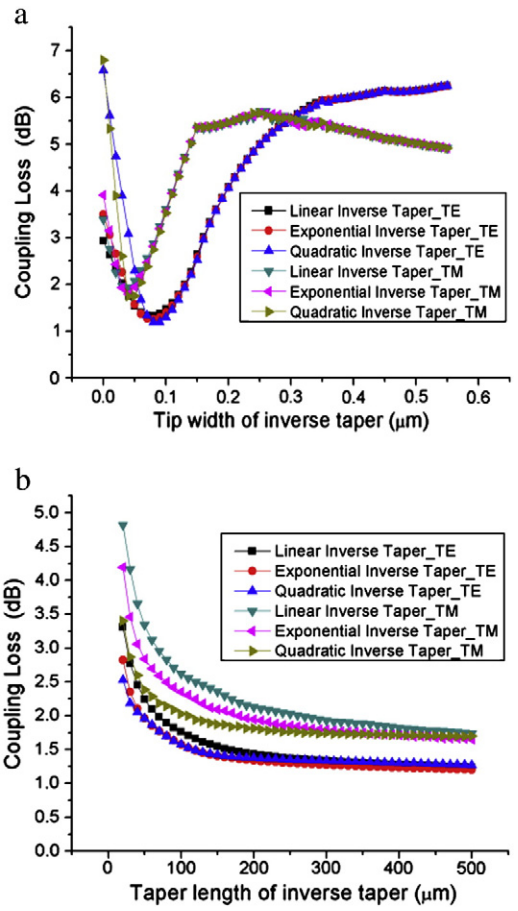


**Fig. 12.** The effect of inverse taper gradient line shape function (a) 300μm long inverse taper with varied tip width (b) 0.07μm tip width for TE mode and 0.04μm tip width for TM mode with varied taper length.

propagation loss exceeds the mode mismatch loss. However, the fabrication tolerance is quite tight when tip width is less than 0.08 μm; most of the inverse taper tip reported up to now is larger than 0.08 μm. When the tip width is larger than 0.08 μm for TE mode (0.04 μm for TM mode) the best coupling case is replaced by quadratic inverse taper, followed by exponential and linear inverse taper, where the mode mismatch loss surpasses the propagation loss. Besides, when the coupling loss reaches the same level, for illustration 1.5 dB for TE mode, the taper tip width for exponential inverse taper (0.11 μm) and quadratic inverse taper (0.115 μm) are larger

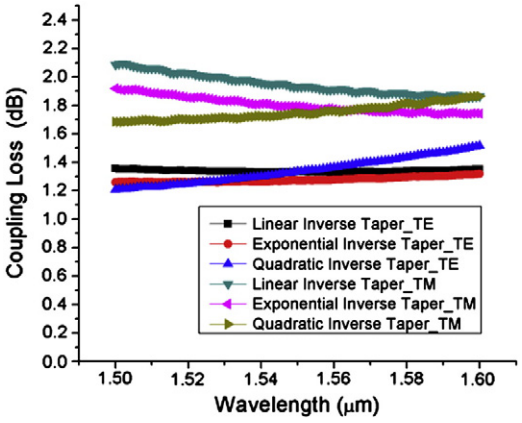


**Fig. 13.** Operation bandwidth of three inverse tapers.

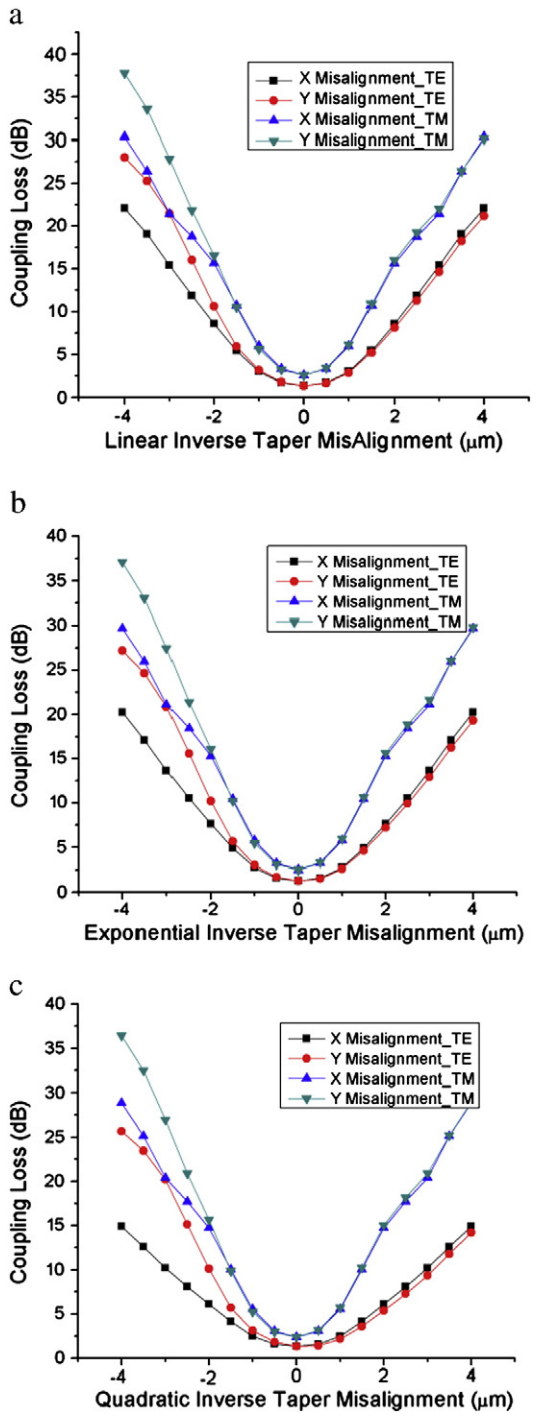


**Fig. 14.** Misalignments tolerance of three inverse tapers (a) linear inverse taper (b) exponential inverse taper (c) quadratic inverse taper.

than that for linear inverse taper (0.1 μm), which is 10% and 15% improvement over the linear inverse taper respectively for fabrication tolerance. This is because of that at the same length the field delocalization of exponential inverse taper and quadratic inverse taper is stronger than that of linear inverse taper, which means the field can expand to a specific size with a larger taper tip width.

From Fig. 12(b), we can see that with the fixed tip width 0.08 μm for TE mode (0.04 μm for TM mode) the coupling loss of exponential and quadratic inverse tapers are lower than that of linear inverse taper at any taper length for TE mode (for TM mode the coupling loss of exponential and quadratic inverse taper are always lower than that of linear inverse taper). At the fixed coupling loss, i.e. 2 dB for TM mode, the taper length for exponential inverse taper (170 μm) and quadratic inverse taper (110 μm) is much shorter than that for linear inverse taper (260 μm), which is 53% and 136% improvement over the linear inverse taper for the reduction of device size. This difference is owing to the fact that the field delocalization of exponential and quadratic inverse taper is much faster than that of linear inverse taper, which means that exponential and quadratic inverse taper can enlarge the field to a specific size in much shorter distance than linear inverse taper does.

(4) Operation bandwidth

Fig. 13 illustrates the operation bandwidth of three inverse tapers. From this graph, we can see that in the 100 nm (from 1500 nm to 1600 nm) range the coupling loss fluctuation is only 0.06 dB for linear inverse taper for TE mode (0.23 dB for TM mode), 0.06 dB for exponential inverse taper for TE mode (0.18 dB for TM mode) and 0.31 dB for quadratic inverse taper (0.18 dB for TM mode). In this aspect, exponential and quadratic inverse taper show no significant advantages over linear inverse taper. With such low coupling loss fluctuation in a wide operation wavelength range of 100 nm, it is good enough to put such mode transformers into practice.

(5) Misalignment tolerance

In this section, we fixed the tip width at 0.08 μm for TE mode (0.04 μm for TM mode) and taper length at 300 μm. The coupling loss caused by misalignments both in horizontal (X-direction) and vertical (Y-direction) directions is studied for three types of inverse tapers respectively.

Fig. 14 tells us that when the additional coupling loss is 3 dB for linear inverse taper the misalignment tolerance in X direction is ±1.27 μm for TE mode (±0.93 μm for TM mode), while in Y direction is ±1.21 μm for TE mode (±0.98 μm for TM mode), for exponential inverse taper the misalignment tolerance in X direction is ±1.35 μm for TE mode (±0.94 μm for TM mode), while in Y direction is ±1.24 μm for TE mode (±1 μm for TM mode) and for quadratic inverse taper the misalignment tolerance in X direction is ±1.56 μm for TE mode (±0.96 μm for TM mode), while in Y direction is ±1.24 μm for TE mode (±1.03 μm for TM mode). The misalignment tolerance improvement of exponential and quadratic inverse taper over the linear inverse taper is 6% and 23% for TE mode at the X direction. Besides, from this figure, we can see that the misalignment tolerance for TM mode is smaller than that for TE mode for all the three inverse tapers. This is because that the field delocalization in X direction (also the TE mode field direction) is stronger than that in Y direction (also the TM mode field direction), in which the inverse taper has a fixed height. It is the strong delocalization effect of inverse taper that contributes to the large misalignment tolerance, which is big enough for easy coupling operation.

## 5. Conclusion

We have studied the factors that affect the performances of inverse tapers, including tip width, taper length, taper shape function, wavelength and misalignment. From the comparison of three types of inverse taper we can draw the conclusion that although exponential and quadratic inverse tapers are marginally better than linear inverse taper in coupling efficiency, their device size, fabrication intolerance and misalignment tolerance at the same coupling loss level perform much better than that of linear inverse taper. Therefore, it is better to adopt the exponential or quadratic inverse taper instead of the commonly used linear inverse taper in our following device fabrication.

## Acknowledgements

This work is supported by the State Key Development Program for Basic Research of China (No. 2007CB613405), and the National Natural Science Foundation of China (No. 60877013 and No. 60837001).

## References

[1] G. Roelkens, D. Vermeulen, D. Van Thourhout, R. Baets, S. Brision, P. Lyan, P. Gautier, J.-M. Fédéli, Appl. Phys. Lett. 92 (2008) 13110.
[2] Taillaert Dirk, Frederik van Laere, Ayre Melanie, Bogaerts Wim, Dries van Thourhout, Bienstman Peter, Baets Roel, Jpn. J. Appl. Phys. Vol. 45 (No. 8A) (2006) 6071.
[3] G. Roelkens, D. Vermeulen, F. Van Laere, S. Selvaraja, S. Scheerlinck, D. Taillaert, W. Bogaerts, P. Dumon, D. Van Thourhout, R. Baets, J. Nanosci. Nanotechnol. 10 (3) (2010) 1551.
[4] S. Scheerlinck, J. Schrauwen, F. Van Laere, D. Taillaert, D. Van Thourhout, R. Baets, Opt. Express 15 (15) (2007) 9625.
[5] F. Van Laere, T. Claes, J. Schrauwen, S. Scheerlinck, W. Bogaerts, D. Taillaert, L. O'Faolain, D. Van Thourhout, R. Baets, IEEE Photonics Technol. Lett. 19 (23) (2007) 1919.
[6] F. Van Laere, Maria V. Kotlyar, D. Taillaert, D. Van Thourhout, Thomas F. Krauss, R. Baets, IEEE Photonics Technology Letters 19 (6) (2007) 396.
[7] Goran Z. Masanovic, Vittorio M.N. Passaro, Graham T. Reed, J. Lightwave Technol. 15 (10) (2003) 1395.
[8] Lu Zhaolin, Dennis W. Prather, Opt. Lett. 29 (15) (2004) 1748.
[9] A. Delage, S. Janz, D.X. Xu, D. Dalacu, B. Lamontagne, A. Bogdanov, Proc. of SPIE, Vol. 5577, SPIE, Bellingham, WA, (2004) 204.
[10] V.R. Almeida, R.R. Panepucci, M. Lipson, Opt. Lett. 28 (2004) 1302.
[11] Kevin K. Lee, Desmond R. Lim, Pan Dong, Hoepfner Christian, Wang-Yuhl Oh, Opt. Lett. 30 (5) (2005) 498.
[12] Tsuchizawa Tai, Yamada Koji, Watanabe Toshifumi, Fukuda Hiroshi, Nishi Hidetaka, Hiroyuki Shinojima, Itabashi Seiichi, Proceeding of Group IV Photonics, 5th IEEE international Conference. Sorrento, Italy, (2008) 200.
[13] G. Roelkens, P. Dumon, W. Bogaerts, IEEE Photonics Technol. Lett. 17 (12) (2005) 2613.
[14] Liu Yan, Li Yan, Fan Zhongchao, Xing Bo, Yu Yude, Yu Jinzhong, J. Opt. A: Pure Appl. Opt. 11 (2009) 085002 (4pp).
[15] N. Yoshimoto, K. Kawano, H. Takeuchi, S. Kondo, Y. Noguchi, Electron. Lett. 28 (17) (1992) 1610.
[16] T. Shoji, T. Tsuchizawa, T. Watanabe, K. Yamada, H. Morita, Electron. Lett. 38 (25) (2002) 1669.
[17] Sure Anita, Dillon Thomas, Murakowski Janusz, Lin Chunchen, Pustai David, Dennis W. Prather, Opt. Exp. 11 (26) (2003) 3555.
[18] P.-C. Lee, E. Voges, J. Light. Technol. 12 (2) (1994) 215.
[19] G. Paul, J.R. Suchoski, Ramu V. Ramaswamy, IEEE J. Quantum Electron. QE-23 (NO.2) (1987) 205.